Transactions, SMiRT-25
Charlotte, NC, USA, August 4-9, 2019
Division V

A CYCLIC BACKBONE CURVE FOR REINFORCED CONCRETE SHEAR WALLS AT ELEVATED TEMPERATURES

Alok A. Deshpande[1], Andrew S. Whittaker[2]

[1] Research Engineer, Department of Civil, Structural and Environmental Engineering, University at Buffalo, Buffalo, NY, USA (alokabha@buffalo.edu)
[2] SUNY Distinguished Professor and MCEER Director, Department of Civil, Structural and Environmental Engineering, University at Buffalo, Buffalo, NY, USA

ABSTRACT

Low aspect ratio reinforced concrete (RC) walls are used in nuclear power plants (NPP) to resist gravity and lateral forces, and to serve a confinement function. Analysis of such walls in NPPs should utilize a cyclic backbone curve similar to that provided in ASCE/SEI Standard 41, with coordinates presented in the peer-reviewed literature, all developed from test data collected at room temperature. Loss of coolant accidents in containment structures of large light water nuclear reactors can result in internal temperatures of up to 300°F [149°C] but the effects of such temperatures on the response of RC shear walls is unknown. To fill this gap in the knowledge, tests on materials and structural components at elevated temperatures were performed. In the materials tests, concrete cylinders were tested in the residual condition after being subjected to elevated temperature of up to 600°F [316°C]. The effects of temperature on uniaxial compressive strength and dynamic modulus of elasticity of concrete were measured. In the component tests, fully reversed, in-plane, inelastic cyclic loading was imposed on four planar walls in ambient and heated conditions to measure the effects of elevated temperature on stiffness and peak strength. The walls had web reinforcement ratios of 0.93% and 2%; concrete compressive strength was approximately 6 ksi [41 MPa]. The maximum surface temperature for the wall tests was 450°F [232°C], which is higher than the temperatures identified in design control documents for new NPP designs. After exposure to elevated temperature of up to 450°F [232°C], the materials tests on concrete showed a reduction in dynamic modulus and uniaxial compressive strength of approximately 30% and 10%, respectively. The key conclusions from the wall tests were that: 1) for levels of force less than about 30% of peak lateral strength, the maximum reduction in stiffness due to exposure to elevated temperature of up to 450°F [232°C], is 30%; 2) for levels of force approaching peak lateral strength, any reduction in stiffness due to exposure to elevated temperature of up to 450°F [232°C] is masked by mechanical damage and can be ignored; and 3) exposure to temperature of up to 450°F [232°C] will not affect wall strength in a meaningful way. Recommendations are provided to modify the cyclic backbone curve for low aspect ratio walls in ASCE 41-17 to address analysis at temperatures up to 450°F [223°C].

INTRODUCTION

Reinforced concrete (RC) walls are used in nuclear power plants (NPP) to resist gravity and lateral forces, and some serve a confinement function. The aspect ratio of many RC walls in NPPs is less than one and the cyclic response is dictated by shear force, namely, the walls are shear critical. Lateral load – deformation relationships (also known as cyclic backbone curves) of walls are needed for analysis of NPPs subjected to design basis and beyond design basis earthquake shaking. ASCE/SEI Standard 41-17 (ASCE, 2017), provides such curves for modeling reinforced concrete components. For shear critical walls, the standard presents a bilinear-to-peak force-drift relationship, which is reproduced in Figure 1. Point *F* in Figure 1 is

associated with the onset of cracking in the wall, which is assumed to correspond to an average shear stress of approximately $4\sqrt{f_c}$ in psi units. Updated values of the coordinates for shear-critical walls are provided in Epackachi et al. (2019) and Chapter 8 of NIST GCR-17-917-45 (NIST, 2017), all of which are based on analysis of data from tests performed at room temperature.

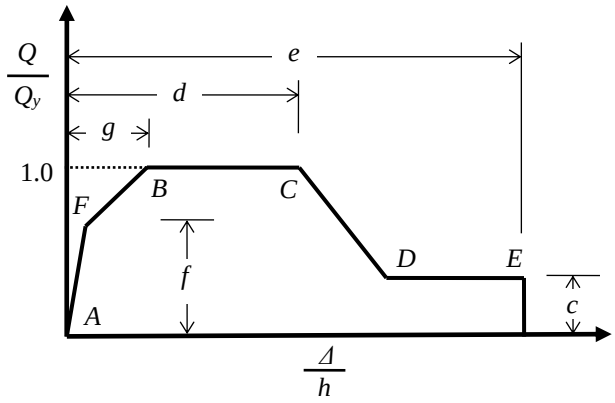

Figure 1: Generalized force–drift ratio relationship for shear critical RC walls (ASCE, 2017).

Loss of Coolant Accidents (LOCA) in nuclear power plants are "…accidents that result in a loss of reactor coolant at a rate in excess of the capability of the reactor makeup system from breaks in the reactor coolant pressure boundary, up to and including a break equivalent in size to the double-ended rupture of the largest pipe of the reactor coolant system" (NRC, 2018). Water is the coolant in Boiling Water Reactors (BWR) and Pressurized Water Reactors (PWR). A LOCA in a BWR or a PWR could result in the release of high-pressure, high-temperature steam into the airtight containment structures of these reactors. Design Control Documents (DCD) filed with the United States Nuclear Regulatory Commission (GEH, 2014; GENE, 1997; WEC, 2011) provide thermal histories that may result from a LOCA. A maximum temperature of approximately 300°F [149°C] is anticipated in a worst-case scenario and it may persist for at least 72 hours after an accident. In the event of a LOCA in a NPP, which could be triggered by earthquake shaking, one important question must be addressed, namely, has the integrity of the RC walls in the vicinity of the pipe break been meaningfully compromised by exposure to elevated temperature? If the answer is yes, the affected walls may have to be demolished and replaced to restore design-basis strength. If the answer is no, a reactor restart may be possible immediately after the failed pipe has been replaced, with no remedial work required for the exposed walls.

The effects of temperature up to 450°F [223°C] on the stiffness and strength of RC walls were measured through a first-of-a-kind experimental study. The foci were lateral stiffness to peak strength (point *B* in Figure 1) and peak strength. Materials studies were performed to measure the effects of elevated temperature on the concrete used to cast the walls. The experimental program and key results are presented in this paper. Recommendations for nonlinear analysis of RC walls subjected to elevated temperatures are provided. Much additional information is available in Deshpande (2019) and Deshpande and Whittaker (2019).

EXPERIMENTAL PROGRAM

Four planar, rectangular RC structural walls (denoted as W1 to W4) were constructed and subjected to cyclic inelastic mechanical loading at temperatures of up to 450°F [223°C]. The walls were 60 inches [1.52 m] long and 10 inches [0.25 m] thick. Grade 60 rebar conforming to ASTM A706 (ASTM, 2016) was used in all walls. Two walls (W1 and W4) had web reinforcement ratios of 0.93% in the horizontal and vertical

directions, and two walls (W2 and W3) had web reinforcement ratios of 2% in the horizontal and vertical directions. The wall and its foundation were cast at the same time, with no construction joint. Pre-test calculations were performed to estimate the capacities of the walls to design the foundation assembly and the test fixture. The calculations indicated that walls W1 and W4 (0.93% web reinforcement ratio) would likely fail in flexure/shear and walls W2 and W3 (2% web reinforcement ratio) would fail in shear.

Loading and heating apparatus

In-plane lateral loads were applied to each wall using two hydraulic cylinders units that operated in force control only. Each load cycle was identified by either a target force or a target displacement. A target displacement was achieved by incrementing load until the desired value was achieved. The hydraulic units imposed forces on the wall specimen via clevises and I-shaped structural steel sections that were post-tensioned to each side of the wall. The distance between the top of the foundation and centerline of loading was 37 inches [0.94 m]. No axial load was applied to the walls.

The walls were heated using radiant heating panels. Two pairs of four heating panels each were used to heat the wall from both sides. Each panel was rated at 6 kW and was controlled independently using a manufacturer-supplied system, with feedback from thermocouples installed on the wall surface. Photographs of the test setup, showing the loading and heating assemblies, are presented in Figure 2.

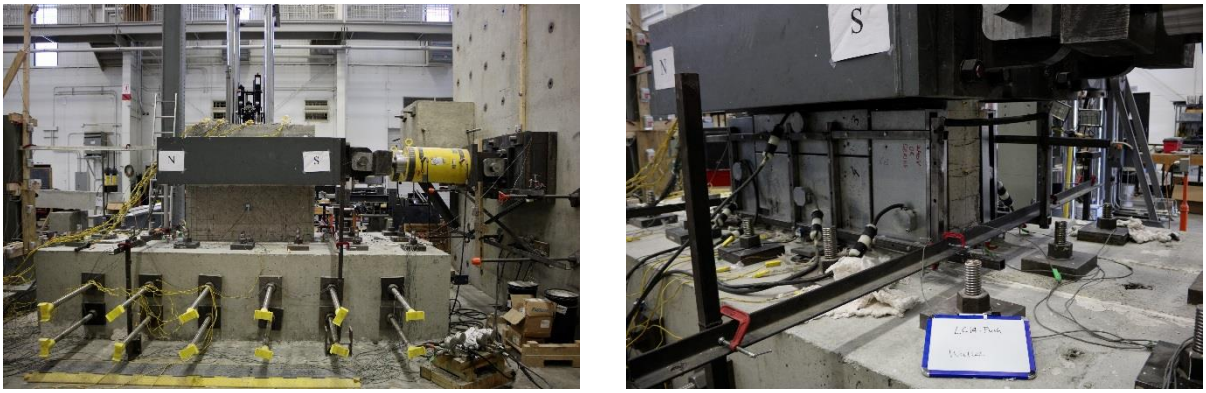

(a) Test setup showing the loading assembly (b) Heater assembly installed on a wall

Figure 2. Wall test setup.

Instrumentation

Linear potentiometers and string potentiometers were used to measure the in-plane and out-of-plane displacements of each wall, and sliding and uplift of the foundation assembly. Gages, capable of measuring 15% strain at temperatures of up to 572°F [300°C], were installed on horizontal and vertical rebar in each wall. Type-K thermocouples, capable of measuring temperatures between -328°F [-200°C] and 2282°F [1250°C], were installed in each wall specimen. Four sets of five thermocouples each, measured the thermal gradient through the wall and were installed prior to casting of concrete. Sixteen thermocouples measured the temperature on the wall surfaces, and were installed after formwork had been stripped.

Materials

One concrete mix design was used for all four walls, but the day-of-test compressive strength varied between 5.6 ksi [38.6 MPa] and 6.5 ksi [44.8 MPa] because the walls were not tested at the same number of days after casting. Calcareous coarse aggregate (sourced from a limestone quarry in Indiana) and river

sand (available locally to West Lafayette, Indiana), were used in the concrete. Type-I cement conforming to ASTM C150 (ASTM, 2017a) was used. The proportions (by weight) of coarse aggregate, sand, and water used in the concrete were 3.28, 2.62 and 0.45, respectively, with respect to the weight of cement.

Although ACI 216.1-14 (ACI, 2014) and Eurocode 2 (CEN, 2004) provide empirical relationships for variation of concrete strength with temperature, the underlying data are highly scattered (Naus, 2010) due to incomplete test descriptions, varying heating and testing protocols, and different types of specimens (Schneider, 1988). Accordingly, materials tests were performed on the concrete used to cast the walls to aid the interpretation of results and make recommendations for design.

Cylinders, 3 inches [76 mm] in diameter and 6 inches [152 mm] in length, were cast using concrete with the same mix proportions and the same aggregates used to cast the walls. Control cylinders were tested at room temperature (20°C), and the remaining cylinders were heated to 212°F [100°C], 250°F [121°C], 300°F [149°C], 450°F [223°C] or 600°F [316°C]. The cylinders were heated in a box furnace at a rate of 7°F/min [4°C/min] till they reached the target temperature, were kept at the target temperature for 90 minutes, cooled naturally inside the furnace and then tested within 24 hours of cooling to room temperature. The cylinders were tested in the residual condition; the dynamic modulus and uniaxial compressive strength were measured. Because the mechanical properties of steel are not affected substantially up to 450°F [223°C] (CEN, 2004), which was the maximum temperature applied in the wall tests, materials tests on rebar at elevated temperature were not performed.

Table 1 summarizes important information on the four walls: web reinforcement ratio, the age of the wall on the first day of testing, duration of testing, first day-of-test concrete compressive strength (f_c), shear stress in the wall in the first load cycle (LC1) as a function of the square-root of f_c, estimated lateral strength and mode of failure. Methods used to calculate lateral strength are provided in Deshpande (2019).

Table 1: Summary data on the walls.

Wall	Web reinf.	Age at start of testing (days)	Duration of testing (days)	Comp. strength of conc. at start of testing, f_c (ksi) [MPa]	Shear stress in LC1 as a factor of $\sqrt{f_c}$ $\left(\sqrt{\text{psi}}\right)$ $\left[\sqrt{\text{MPa}}\right]$	Est. lateral strength (kips) [kN]	Exp. mode of failure
W1	0.93%	86	12	6.3 [43.4]	1.7 [0.14]	275 [1224]	Flexure
W2	2.0%	52	13	6.0 [41.4]	1.7 [0.14]	460 [2047]	Shear
W3	2.0%	108	6	5.6 [38.6]	1.8 [0.15]	440 [1958]	Shear
W4	0.93%	109	3	6.5 [44.8]	1.6 [0.13]	275 [1224]	Flexure

RESULTS AND DISCUSSION

Materials tests

The materials tests were performed about 30 days after cylinders were cast. The uniaxial compressive strength and dynamic modulus of the control cylinders at room temperature were 5.3 ksi [36.5 MPa] and 5,300 ksi [36.5 GPa], respectively. The variations in dynamic modulus and uniaxial compressive strength

with temperature, from testing in the residual condition, are presented in Figure 3. The dynamic modulus elasticity of the cylinders, E_c, was measured at room temperature, in accordance with ASTM C215 (ASTM, 2014), before and after heating. Tests performed by Phan and Carino (2002) indicated that the percentage reduction in dynamic modulus of concrete with increasing temperature is similar to the reduction in static modulus. Accordingly, the relation provided by CEB (1991) for variation of static modulus of concrete with temperature is also plotted in Figure 3 (a). The uniaxial compressive strength of the cylinders, f_c, was measured in accordance with ASTM C39 (ASTM, 2017b). The variation of concrete strength with temperature recommended by CEB (1991) and Eurocode 2 (for concrete made with calcareous aggregate) (CEN, 2004) are plotted in Figure 3 (b) for information. The trends in the data from the materials study are in good agreement with those of CEB and Eurocode 2. The modulus of elasticity and uniaxial compressive strength of concrete reduce by approximately 30% and 10%, respectively, after exposure to 450°F [223°C].

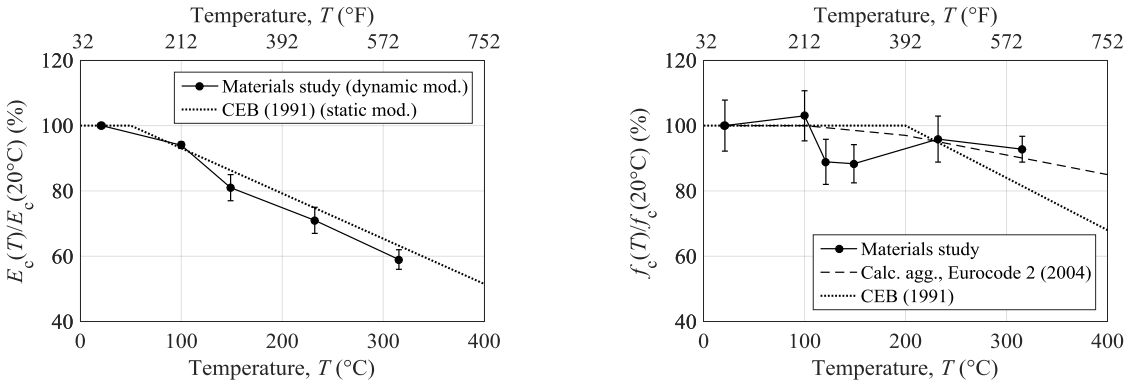

(a) Modulus of elasticity (b) Uniaxial compressive strength

Figure 3. Variation of mechanical properties of concrete with temperature, normalized with values at room temperature.

Wall tests

The initial stiffness of each wall was measured at room temperature, before heat was applied, at a force corresponding to approximately 25% of the estimated peak lateral strength. The values of secant stiffness were approximately 30% of the theoretical uncracked value, calculated using strength of mechanics equations and day-of-test compressive strength of concrete. The reduction in stiffness from the uncracked value is attributed primarily to restrained shrinkage at the base of the wall, near the wall-foundation junction. Strain gage measurements on the vertical rebar at the base of the wall indicated cracking in the first load cycle (LC1), performed at forces corresponding to shear stress substantially less than $4\sqrt{f_c}$ (psi units) that is linked to cracking in ACI 318-14. This observation is consistent with that reported first by Sozen and Moehle (1993) and later confirmed by Luna et al. (2015).

Unique heating and loading protocols were applied to each wall, and these are summarized below. Additional details are provided in Deshpande (2019) and Deshpande and Whittaker (2019). The global force – drift ratio relationships, and the temperature measured through the thickness of the wall at representative locations, is presented in Figure 4. Surface temperatures are not plotted in Figure 4.

Wall1

Two loading cycles (LC1 and LC2) were performed at room temperature, at lateral forces corresponding to approximately 25% and 40% of the estimated peak lateral strength. The wall was heated to a target surface temperature of 300°F [149°C] after LC2, and load cycles LC1 and LC2 were repeated in the heated condition, and designated as LC3 and LC4. The displacement at the centerline of loading at peak lateral resistance in LC4 was designated as the reference displacement, d*. Further cycles were applied in the heated condition in increments of d*. Two cycles were performed at each target displacement until the strength of the wall in heated condition had been reached, which occurred in LC15. The heaters were switched off after LC15, and subsequent cycles were applied in increments of d* (starting at displacement applied in LC15) after the wall cooled to room temperature, until the wall *failed*.

The temperature at the center of the wall at the start of LC3 (first heated cycle) and LC15 (last heated cycle) was approximately 100°F [38°C] and 230°F [110°C], respectively. The secant stiffness in load cycle performed at elevated temperature to a force level of about 40% of peak strength (LC4) was approximately 20% less than the value for the load cycle performed to the same force level at room temperature (LC2). No significant differences in the values of secant stiffness were observed for the load cycles performed to the same displacement in subsequent cycles (LC5 to LC15). Accordingly, the reduction in stiffness from LC2 to LC4 is attributed to cracking due to thermal effects. The peak lateral strength measured in the heated condition (LC15) and the residual condition was approximately 270 kips [1201 kN], which is within 5% of the estimated lateral strength at room temperature. The secant stiffness reduced at the larger displacements applied in later cycles, and the wall *failed* at a drift ratio of approximately 1.8%.

Wall 2

Four loading cycles were performed at room temperature, at lateral forces corresponding to approximately 15% (LC1), 25% (LC2 and LC3) and 40% (LC4) of the estimated peak lateral strength. The wall was heated to a target surface temperature of 450°F [223°C] after LC4, and two cycles were performed at a force corresponding to LC4, after two periods of heating: 15 minutes (LC5) and 2 hours (LC6). The surfaces of the wall were maintained at the target temperature of 450°F [223°C] between LC5 and LC6. The displacement at the centerline of loading at peak lateral resistance in LC6 was designated as the reference displacement, d*. The heaters were removed after LC6 and the wall cooled naturally to room temperature. This heating and testing protocol was repeated at greater displacements: two cycles were performed at the each displacement level after two periods of heating (15 minutes and 2 hours), until the strength of the wall in the heated condition had been reached, which occurred in LC16. One subsequent loading cycle (LC17) was applied in the residual condition at the target displacement of LC16, during which the wall *failed*.

The temperature at the center of the wall at the start of each cycle, performed after 15 minutes and 2 hours of heating, was approximately 100°F [38°C] and 230°F [110°C], respectively. No significant differences in stiffness were observed in the loading cycles to the same displacement performed after 15 minutes and 2 hours of heating. The peak lateral strengths at elevated temperature (LC15) and room temperature (LC17) were approximately 450 kips [2003 kN] and 460 kips [2046 kN], respectively. These values are within 5% of the estimated lateral strength at room temperature. The wall *failed* at a drift ratio of approximately 1.4%.

Wall 3

Two cycles (LC1 and LC2) were performed at room temperature, at lateral forces corresponding to approximately 15% and 25% of the estimated peak lateral strength. The wall was heated to a target surface temperature of 300°F [149°C] after LC2, and one load cycle (LC3) was performed to the same maximum force of LC2 15 minutes after the surface reached the target temperature. The heaters were switched off

after LC3 and the wall cooled naturally to room temperature. One load cycle (LC4) was performed at room temperature at a lateral force corresponding to approximately 40% of the estimated peak lateral strength. Two load cycles were performed to the same force level as LC4, at surface temperatures of 300°F [149°C] (LC5) and 450°F [223°C] (LC6). Load cycles LC5 and LC6 were performed 15 minutes after the surface of the wall had reached the target temperature. The heaters were removed after LC5. Heating for LC6 began after the wall had cooled naturally to room temperature. The displacement at the centerline of loading at peak lateral resistance in LC6 was designated as the reference displacement, d*. The heaters were kept on after LC6 and the wall surfaces were maintained at 450°F [223°C]. Subsequent cycles were applied in increasing increments of d*, with two cycles at each displacement, until the strength of the wall was reached at elevated temperature, which occurred in LC15. The heaters were then switched off and the wall cooled naturally to room temperature. Subsequent cycles were applied at room temperature in increments of d*, starting at displacement applied in LC15, until the wall *failed*.

The secant stiffness of the wall in LC3 was approximately 20% less than the value in LC2. Load cycles LC2 and LC3 were performed to a force corresponding to approximately 25% of the lateral strength. No significant differences in stiffness were observed in subsequent loading cycles performed to the same displacement. Accordingly, the reduction in stiffness from LC2 to LC3 is attributed to cracking due to thermal effects. The peak lateral strengths measured at elevated temperature (LC15) and room temperature (LC18) were approximately 445 kips [1980 kN] and 455 kips [2025 kN], respectively. These values are within 5% of the estimated lateral strength at room temperature. The wall *failed* at a drift ratio of approximately 1.5%.

Wall 4

One load cycle (LC1) was performed at room temperature at a lateral force corresponding to approximately 25% of the estimated peak lateral strength. The wall was heated after LC1 to a target surface temperature of 450°F [223°C] and two cycles were performed at a force corresponding to LC1, 15 minutes (LC2) and 2 hours (LC3) after the wall surface reached the target temperature. The wall surfaces were maintained at the target temperature between LC2 and LC3. The heaters were removed after LC3 and the wall cooled naturally to room temperature. One load cycle (LC4) was performed at room temperature at a force corresponding to approximately 40% of the estimated peak lateral strength. The wall was heated after LC4 to a target surface temperature of 450°F [223°C], and two cycles were performed at a force corresponding to LC4, 15 minutes (LC5) and 2 hours (LC6) after the wall surface reached the target temperature. The wall surfaces were maintained at the target temperature between LC5 and LC6. The displacement at the centerline of loading at peak lateral resistance in LC6 was designated as the reference displacement, d*. The heaters were kept on after LC6 and the wall surfaces were maintained at 450°F [223°C]. Subsequent cycles were performed in increasing increments of d*, two cycles at each displacement, until the strength of the wall was reached, which occurred in LC18. The heaters were then switched off, and the wall cooled naturally to room temperature. Subsequent cycles were applied at room temperature in increments of d* (starting at displacement applied in LC18) until the wall *failed*.

The secant stiffness of the wall in LC2 (performed 15 minutes after the wall surface reached a target surface temperature of 223°C) was approximately 30% less than the value in LC1 (performed at the same force level as LC2 at room temperature). Load cycles LC1 and LC2 were performed to a force corresponding to approximately 25% of the lateral strength. No significant differences in lateral stiffness were observed in subsequent loading cycles to the same displacement. Accordingly, the reduction in stiffness from LC1 to LC2 is attributed to cracking due to thermal effects. The peak lateral strengths at elevated temperature (LC13) and room temperature (LC18) were approximately 245 kips [1090 kN] and 260 kips [1157 kN], respectively, and are within 5% of the estimated lateral strength at room temperature. The wall *failed* at a drift ratio of approximately 2%.

Wall	Global force – drift ratio relationship	Temperatures measured in heated cycles
W1	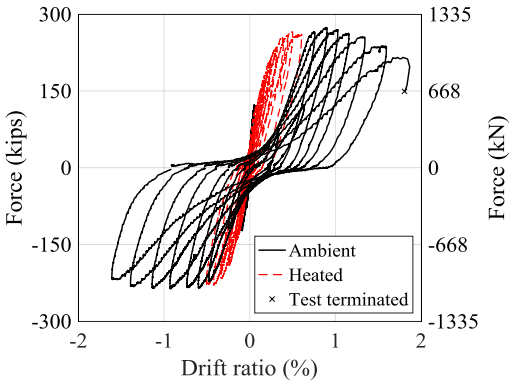	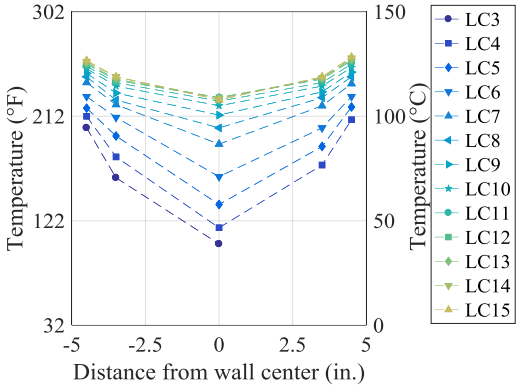
W2	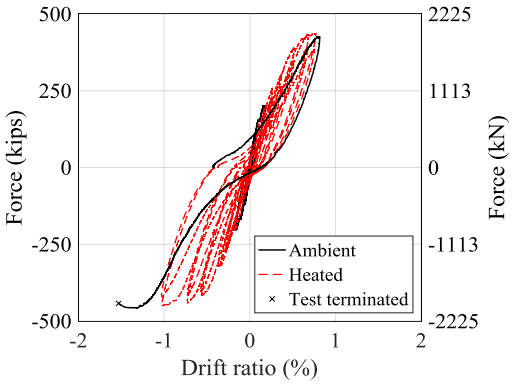	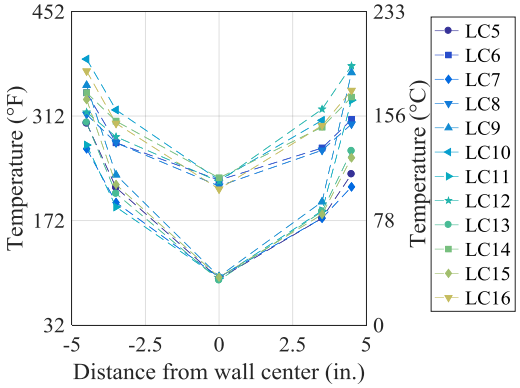
W3	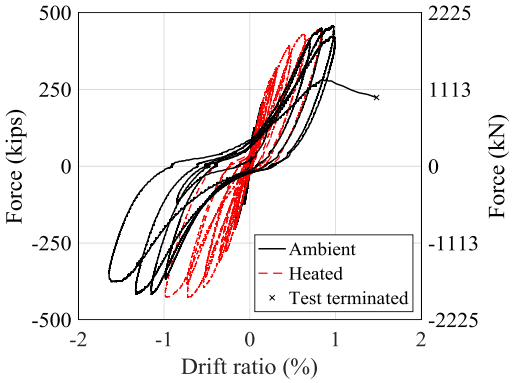	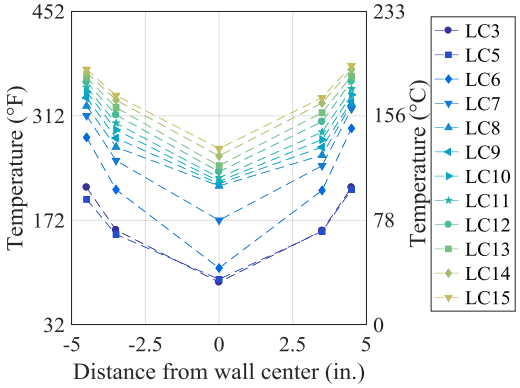
W4	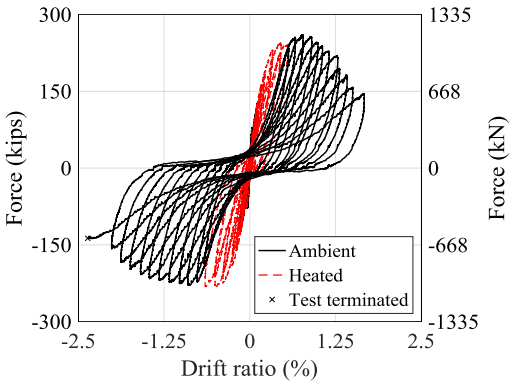	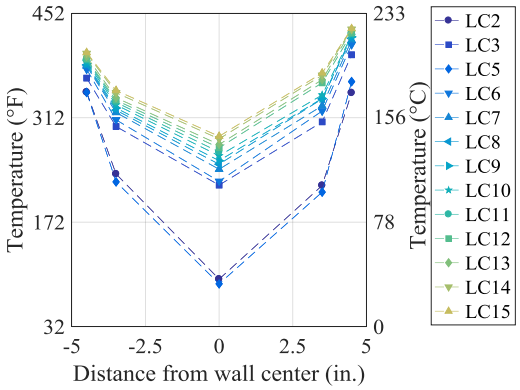

Figure 4. Summary of wall test data.

SUMMARY AND CONCLUSIONS

Thermal accidents resulting from steam pipe-breaks in containment structures in a large light water reactors can result in internal temperatures of up to 300°F [149°C]. The effects of exposure to temperatures up to 450°F [223°C] on the mechanical behavior of concrete, and stiffness and strength of low aspect ratio, planar reinforced concrete structural walls, were investigated through materials and component testing. The key conclusions are:

1. The initial stiffness of walls tested in the study, and measured at room temperature, was approximately 30% of the theoretical uncracked value calculated using strength of mechanics equations and day-of-test compressive strength of concrete.

2. Exposure to 450°F [223°C] reduces the modulus of elasticity and uniaxial compressive strength of concrete by approximately 30% and 10%, respectively. The reductions are based on the materials tests performed in this study and are similar to those recommended by design codes.

3. The maximum reduction in lateral stiffness of RC walls due to exposure to elevated temperature of up to 450°F [223°C], at levels of force less than about 30% of the peak lateral strength, and in the absence of significant axial compression, is 30%. At levels of force greater than about 30% of the peak lateral strength, the effects of exposure of elevated temperature of up to 450°F [223°C] on lateral stiffness will be masked by mechanical damage, and thermal effects can be ignored.

4. The peak lateral strength of a lightly reinforced wall (strength governed by yielding of reinforcement) is not expected to reduce due to exposure to elevated temperature of up to 450°F [223°C]. For heavily reinforced walls (strength governed by the failure of diagonal compression struts), exposure to 450°F [223°C] can reduce the peak lateral strength by up to 10%.

5. Figure 1 presents the backbone curve for modeling shear critical RC walls. If the goal of analysis is to predict response in the range *AF* at 450°F [223°C], the lateral stiffness should be reduced by 30% from the updated value given in NIST GCR-17-917-45 (NIST, 2017). If the goal of analysis is to predict response in the range *AB* at 450°F [223°C], a linear model *AB* is recommended (i.e., no point *F*), using the updated coordinates for point *B* per the NIST report, with no additional reduction in stiffness due to thermal effects.

ACKNOWLEDGMENTS

The United States Department of Energy (DOE) provided financial support for the wall tests described in this paper. The DOE contract was with Purdue University (Professor Amit Varma, PI) and the University at Buffalo served as a subcontractor to Purdue University for the tests on the reinforced concrete walls. Professor Amit Varma, Dr. Saahastaranshu Bhardwaj and the staff at the Bowen Laboratory at Purdue University contributed in a significant way to the execution of the experiments at Purdue University, and these contributions are gratefully acknowledged. Irving Materials Incorporated (IMI) and LafargeHolcim provided the aggregates and cement, respectively, used in the materials studies reported in this paper. Their support is gratefully acknowledged. The authors thank Dr. Ravi Ranade, undergraduate intern Elliot Whittaker, and the staff of the Structural Engineering and Earthquake Simulation Laboratory at the University at Buffalo for their guidance and assistance with the materials tests.

REFERENCES

American Concrete Institute (ACI). (2014). "Code requirements for determining fire resistance of concrete and masonry construction assemblies (ACI/TMS 216.1-14)." Farmington Hills, MI.

American Society of Civil Engineers (ASCE). (2017). "Seismic evaluation and retrofit of existing buildings (ASCE/SEI 41-17)." Reston, VA.

American Society for Testing and Materials (ASTM). (2014). "Standard test method for fundamental transverse, longitudinal, and torsional resonant frequencies of concrete specimens (ASTM C215-14)." West Conshohocken, PA.

American Society for Testing and Materials (ASTM). (2016). "Standard specification for deformed and plain low-alloy steel bars for concrete reinforcement (ASTM A706/A706M-16)." West Conshohocken, PA.

American Society for Testing and Materials (ASTM). (2017a). "Standard specification for Portland cement (ASTM C150 / C150M-17)." West Conshohocken, PA.

American Society for Testing and Materials (ASTM). (2017b). "Standard test method for compressive strength of cylindrical concrete specimens (ASTM C39/C39M-17b)." West Conshohocken, PA.

Comite Euro-international du Beton (CEB). (1991). "Fire design of concrete structures in accordance with CEB/FIP Model Code 90." Lausanne, Switzerland.

European Committee for Standardization (CEN). (2004). "Eurocode 2: Design of concrete structures. Part 1-2: General rules - Structural fire design (EN 1992-1-2:2004)." Brussels, Belgium.

Deshpande, A. A. (2019). "A multiscale study of concrete subjected to elevated temperatures." Ph.D. Dissertation, State University of New York at Buffalo, Buffalo, NY.

Deshpande, A. A. and Whittaker, A. S. (2019). "Seismic behavior of reinforced concrete walls at elevated temperature." In Press, *ACI Structural Journal*.

Epackachi, S., Sharma, N., Whittaker, A., Hamburger, R. O. and Hortacsu, A. (2019). "A cyclic backbone curve for shear-critical reinforced concrete walls." *Journal of Structural Engineering,* 145(4), 4019006.

GE-Hitachi Nuclear Energy (GEH). (2014). "Design Control Document for Economic Simplified Boiling-Water Reactor (ESBWR)." Agencywide Documents Access and Management System (ADAMS) Accession Number ML14100A493. Nuclear Regulatory Commission (NRC). Washington, DC.

General Electric Nuclear Energy (GENE). (1997). "Design Control Document (DCD) for Advanced Boiling Water Reactor (ABWR)." Agencywide Documents Access and Management System (ADAMS) Accession Number ML11126A100. Nuclear Regulatory Commission (NRC), Washington, DC.

Luna, B. N., Rivera, J. P. and Whittaker, A. S. (2015). "Seismic behavior of low-aspect-ratio reinforced concrete shear walls." *ACI Structural Journal,* 112(5), 593-604.

Naus, D. J. (2010). "A compilation of elevated temperature concrete material property data and information for use in assessments of nuclear power plant reinforced concrete structures." NUREG/CR-7031, Nuclear Regulatory Commission (NRC), Office of Nuclear Regulatory Research, Washington, DC.

National Institute of Standards and Technology (NIST). (2017). "Recommended modeling parameters and acceptance criteria for nonlinear analysis in support of seismic evaluation, retrofit, and design." NIST GCR 17-917-45, Gaithersburg, MD.

Nuclear Regulatory Commission (NRC). (2018). https://www.nrc.gov/reading-rm/basic-ref/glossary/loss-of-coolant-accident-loca.html. *Accessed January 18, 2018.*

Phan, L. T. and Carino, N. J. (2002). "Effects of test conditions and mixture proportions on behavior of high-strength concrete exposed to high temperatures." *ACI Materials Journal,* 99(1), 54-66.

Schneider, U. (1988). "Concrete at high temperatures - a general review." *Fire Safety Journal,* 13(1), 55-68.

Sozen, M. A. and Moehle, J. P. (1993). "Stiffness of reinforced concrete walls resisting in-plane shear." Report No. EPRI TR-102731, Electrical Power Research Institute, Palo Alto, CA.

Westinghouse Electric Company (WEC). (2011). "Design Control Document (DCD) for Advanced Passive 1000 (AP1000) reactor." Agencywide Documents Access and Management System (ADAMS) Accession Number ML11171A303. Nuclear Regulatory Commission (NRC), Washington, DC.